COBEM 2023 27TH INTERNATIONAL CONGRESS OF MECHANICAL ENGENEERING

ABCM Brazilian Society of Mechanical Sciences and Engineering
27th ABCM International Congress of Mechanical Engineering
December 04-08, 2023, Florianópolis-SC, Brazil

COB-2023-0119
INTERFACIAL OSCILLATIONS IN BIDISPERSE BEDS

Vinícius Oliveira
Danilo da Silva Borges
Erick de Moraes Franklin
University of Campinas - r. Medeleyev, 200 - Cidade Universitária, Campinas - São Paulo, Brasil. CEP: 13083-860
v265311@dac.unicamp, proffisicadaniloborges@gmail.com, franklin@fem.unicamp.br

Abstract. *Fluidized beds are described as suspensions of solid grains in a vertical duct by an upward fluid flow. When the ratio between the grain and duct diameters (widths) is less than 10, the bed is classified as very narrow. These kinds of fluidized beds are a novel technology with increasing interest, being used in sediment classifiers and wastewater treatment. However, the state-of-the-art over the last decades dedicated itself to investigating phenomena in monodisperse beds. The addition of another grain type in a fluidized bed would give a better approximation of physical phenomena in real beds, that are actually polydisperse. In this work, we compare the interfacial motion occurring between layers in a bidisperse bed with that at the top of a monodisperse pile. We obtain the amplitude, contribution of each pile in bed height, and relation of mean bed heights for each case. We also compare the velocity fluctuation of particles near the interface with fluctuations far from it. This paper is derived from (Oliveira et al., Accepted).*

Keywords: *Very-narrow fluidized beds, segregation, polydisperse beds, granular matter.*

1. INTRODUCTION

Fluidized beds are suspensions of granular matter that experience an upward flow of fluid. These beds have been extensively applied in various industrial applications for centuries, primarily due to their ability to enhance mass and heat transfer processes (Guazzelli, 2005; Cúñez and Franklin, 2019, 2020; Yao *et al.*, 2021). However, despite their apparent simplicity, fluidized beds exhibit complex physical behavior characterized by intricate particle-fluid and particle-particle interactions. The interaction between particles is of utmost importance in ensuring the proper functioning of the bed, as blockages can disrupt operations, escalate costs, and pose significant risks to industrial processes (Guazzelli, 2005; Yao *et al.*, 2021). Understanding and mitigating these issues is crucial for optimizing the performance and efficiency of fluidized bed systems in industrial settings.

Interactions between particles become particularly significant when the size of the particles is comparable to the size of the bed. Traditional fluidized beds commonly employed in the energy industry typically have a bed-to-particle ratio (D/d) greater than 100. However, in certain applications such as wastewater treatment and sediment classification, it is not feasible to maintain such high ratios. These specific applications impose the use of very-narrow fluidized beds with a ratio of $D/d < 10$. In these narrow beds, the high hindrance and particle concentration give rise to distinct flow regimes, driven by the strong confinement of particles (Cúñez and Franklin, 2019, 2020).

Alternatively, the use of multiple types of particles is encouraging. Processes involving two different types of particles can offer advantages by simultaneously treating both particle types and accelerating the overall process. Besides, sedimenting systems in practical applications are often polydisperse and composed of various particle types (Yao *et al.*, 2021). Additionally, incorporating a layer of smaller particles at the bottom can help prevent blockages in the upper layer. Despite its significance, very-narrow fluidized beds consisting of bidisperse grains have not been the subject of extensive investigation. Over the last decades, however, numerous studies have focused on experimental investigations of regular fluidized beds, with limited numerical research. Richardson and Zaki (1997) conducted a comprehensive experiment to assess the sedimentation velocity in fluidized beds comprising different particle types. They measured the sedimentation velocity of each bed and proposed an empirical correlation. Their findings revealed that the sedimentation velocity v_s is related to the terminal velocity v_t and concentration ϵ, by a constant coefficient $v_s = v_t\epsilon^{2.4}$. In some cases, the aspect ratio can also be incorporated into the coefficient.

Bertho *et al.* (2003) investigated the Janssen effect in dense granular packing under the influence of moving walls. By varying the wall velocities, they observed a variation in the apparent mass of the particles, which remained independent of the velocity when the walls moved upward. The decrease in apparent mass in the final configuration was found to be dependent on velocity, with higher velocities resulting in higher apparent mass. In a recent study, Cúñez and Franklin (2019) conducted experiments and simulations using the CFDDEM method in very narrow fluidized beds. They observed the formation of different patterns and successfully tracked and measured these structures. The experimental and simulation results showed good agreement, providing valuable insights into the behavior of larger particles in fluidized beds.

Goldman and Swinney (2006) investigated glass transitions in narrow fluidized beds. They performed experiments with a square section fluidized bed with 5.81 cm^2 and particles of 250 μm. They observed that the volume fraction has a relation with the motion of the particles and blockage of the bed. They found that as superficial velocity increases, the heterogeneity regions grow. They found that blockage occurs at low deceleration rates of superficial velocity. On the other hand, Cúñez and Franklin (2020) performed experiments in very-narrow fluidized beds and found no relation between deceleration rates and blockages. They found that the blockages occur depending on the kind of particle involved.

Given the unpredictable behavior of such phenomena, experiments, and simulations are necessary to have a better understanding and avoid them. Yao *et al.* (2021) performed simulations using resolved CFDDEM by using immersed boundary method. They formed a bidisperse bed with a square section of 10 $d_{p,1}$ of side, where $d_{p,1} = 0.002$ mm is the diameter of the largest particle. They found that though the segregate layers formed interact by its interface, both layers can be approximated as monodispese ensembles.

This work depicts itself to investigate interfacial interactions in fluidized beds. We present the mean normalized macroscopic characteristics of the bed, oscillations of the interface, and its granular temperature and compare it with the total average granular temperature of the bed. The average interfacial granular temperature is lesser than the bed average granular temperature for all the superficial velocities observed. It indicates that the top bed influences the behavior of the bottom layer, hindering it.

2. METHODOLOGY

The experimental setup consisted of a water tank, a centrifugal pump, a flow meter, a flow homogenizer, a 25.4-mm-ID vertical tube, and a return line. flow rate is controlled by a control unit composed of a frequency inverter, an Arduino UNO, and a flow rate sensor. The fluidized bed is composed of a transparent vertical tube (made of polymethylmethacrylate - PMMA) 1.2 m long, aligned vertically within $\pm$ 3^0. The first 0.65 m corresponds to the test section. A visual box filled with water was placed around the test section to minimize optical distortions. The flow homogenizer consists of a tube (150 mm long) filled with alumina spheres ($d = 6$ mm). These particles are packed between wire screens. Figure 1 shows the layout and a photograph of the experimental setup.

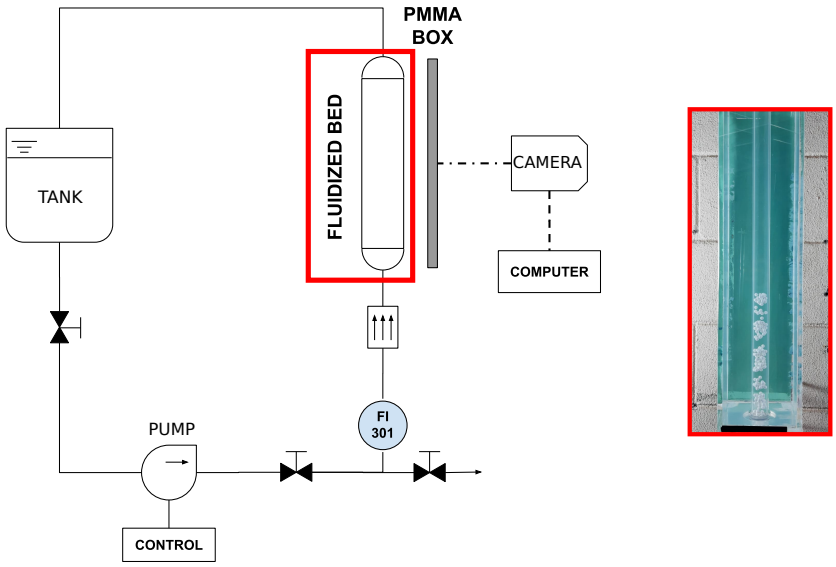

Figure 1. Layout of the experimental setup.

Tap water within 25^{0}C $\pm$ 3^{0}C was used as the fluid (density $\rho_f = 1000$ kg/m^3 and dynamic viscosity $\mu_f = 10^{-3}$ Pa.s). The beds were formed with 0.2 g polymer-covered spheres ($\rho_1 = 1768$ kg/m^3) and diameter $d_1 = 5.95$ mm $\pm$ 0.01 mm, and aluminum spheres ($\rho_2 = 2760$ kg/m^3) with diameter $d_2 = 4.8$ mm $\pm$ 0.03 mm, which we call species 1 and 2, respectively. The species can be seen in Fig. 2. This corresponds to, $D/d_1 = 4.3$ and $D/d_2 = 5.3$, and the numbers of Stokes $St_t = v_t d\rho_p/(9\mu_f)$ and Reynolds $Re_t = \rho_f v_t d/\mu_f$ based on the terminal velocity were, respectively, 404 and 2056 for species 1 and 696 and 2269 for species 2, where v_t is the terminal velocity of one single sphere. The values of St_t and Re_t indicate that the used beads have considerable inertia with respect to water. Prior to each test, grains were let to settle in the test section, forming a granular bed. A bidisperse bed consisting of a top layer with $N_1 = 200$ particles of species 1 and a bottom layer with $N_2 = 300$ particles of species 2 is investigated. With the grains settled, water flows with cross-sectional average velocities U within 0.06 and 0.12 m/s were imposed by controlling the rotation of

the centrifugal pump. For the bed, the average particle fraction ϕ_0 of the settled bed, the heights h_{if} and water velocities U_{if} at the inception of fluidization, and the settling velocity of individual spheres $v_{s,i}$ (for each species) are, respectively, ϕ_0 = 0.469, $h_{if} = 0.062$ m, $U_{if} = 0.05$ m/s, $v_{s,1} = 0.093$ m/s, $v_{s,2} = 0.091$ m/s. Values of $v_{s,i}$ were computed with the Richardson–Zaki correlation, $v_{s,i} = v_t(1-\phi_0)^{2.4}$, and those of ϕ_0, h_{if} and U_{if} were determined experimentally by using image processing, where ϕ_0 is given by h_{if} multiplied by the tube cross-section and divided by the total volume of particles (volume occupied by the solid phase). The total duration of the tests was 300 s.

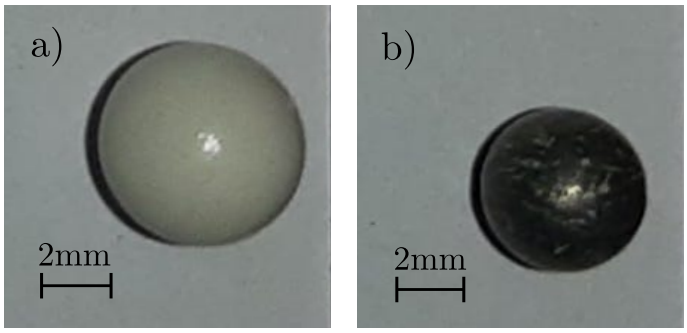

Figure 2. (a) polymer-covered spheres and (b) aluminum spheres used in the experiments.

We made use of digital images in our investigation. For that, we placed a camera of complementary metal-oxide-semiconductor (CMOS) sensor type perpendicularly to the test section. The camera had a resolution of 1920 px $\times$ 1080 px when operating at 60 Hz, and it was connected to a computer that controls both the camera and the pump rotation. We mounted a lens of 60 mm focal distance and F2.8 maximum aperture on the camera and set the camera frequency to 60 Hz and the region of interest (ROI) to 725 px $\times$ 165 px, for a field of view of 111.6 mm $\times$ 25.4 mm. With that, 1 px corresponded to approximately 0.16 mm in our images. In order to have a stable illumination while avoiding undesirable reflections from the tube, we placed a green background, used lamps of light-emitting diode (LED) branched to a continuous-current source, and placed translucent papers just in front of LED lamps. Once acquired and stored, the images were processed with numerical codes written in the course of this work.

3. RESULTS

With image processing, we were able to track macroscopic structures, interface movements, characteristic lengths of these structures, and their celerities. In the bidisperse results shown below, we observe the motion of the interface, and we were able to identify its oscillatory characteristics.

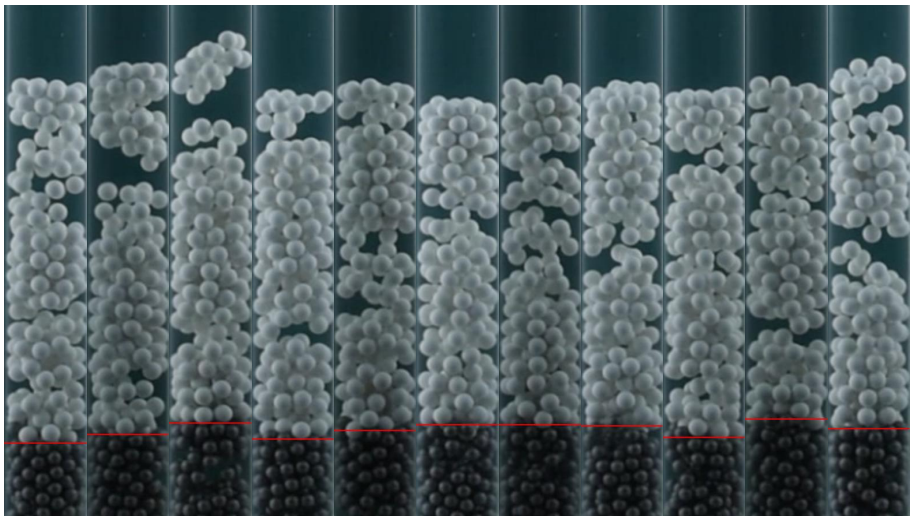

Figure 3. Snapshots showing the interface motion (red line). The time between frames is 4.5 s.

From a macroscopic point of view, we can see the formation of plugs that propagate upward in both layers. Plugs are expected at incipient superficial velocities Cúñez and Franklin (2019); Oliveira *et al.* (2023 (accepted). We measured the bed height H, plug length λ, and plug celerity C, by evaluating the time average of each quantity. In Figure 3 we can observe a clear interface bounding the phases. At this moment, we simplify this interface by a simple line separating the two phases. In Figure 4 we can observe each quantity as a function of superficial velocity and the interface height. Each quantity is normalized by a characteristic quantity of the flow. The bed height rises as the superficial velocity increases.

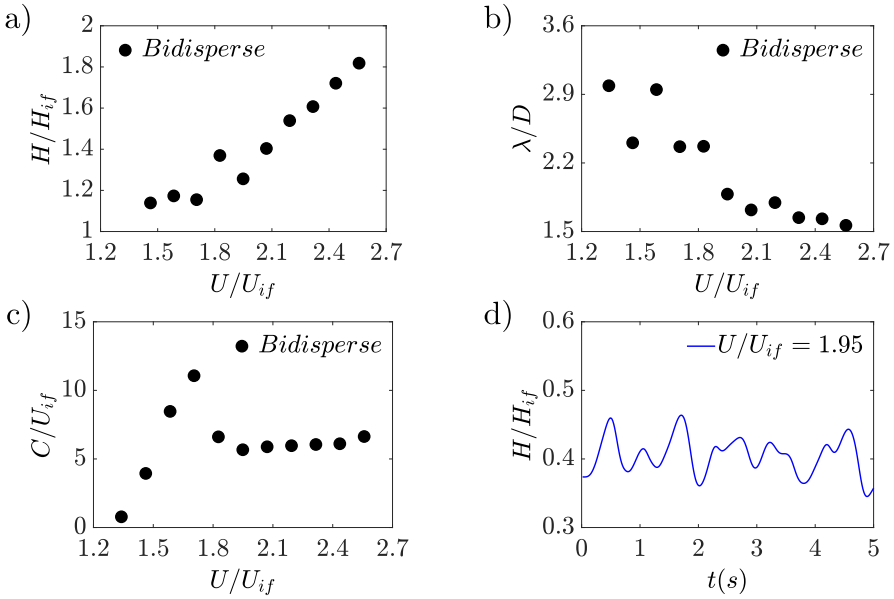

Figure 4. Characteristics of the bidisperse bed. (a) Dimensionless height H/H_{if}; (b) plug length λ/D; and (c) plug celerity C/U_{if} as functions of the dimensionless cross-sectional average velocity U/U_{if}. (d) Time evolution of the interface motion H_I/H_{if}.

It shows the linear expansion of the bed. The plugs are almost independent of the superficial velocity. Finally, celerity presents a nom-monotonical behavior at a range of superficial velocities of 1.50 to 1.80. This transition can be explained by a change of regime at the bottom layer as superficial velocity increases.

We also tracked the individual movement of particles of the whole bed and the interface, measuring the granular temperature. The granular temperature is calculated as in Eq. (1), where $\overline{\theta}$ is the average granular temperature at an instant of time t, $v'_{x,i}$ is the fluctuation of the velocity of the particle i in the horizontal direction, $v'_{y,i}$ is the velocity fluctuation of the particle in the vertical direction and N is the number of visible particles. We calculate both averages and compare them in Fig. 5. We can observe that both averages grow as superficial velocity increases, but the average granular temperature at the interface is lesser than the average granular temperature of the whole bed.

$$\overline{\theta} = \sum_{i=1}^{N} \frac{v'^2_{x,i} + v'^2_{y,i}}{2N} \tag{1}$$

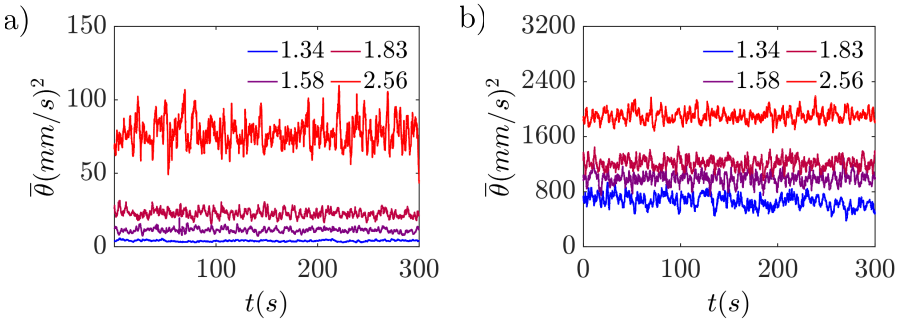

Figure 5. Ensemble-averaged granular temperature $\overline{\theta}$ for (a) the interface and (b) for the whole bed. Captions correspond to values in U/U_{if}.

4. CONCLUSIONS

In this work, we investigated the motion of the interface of a bidisperse bed. We tracked macroscopic quantities, measuring the height of the top layer of the bed height, its plug length, celerity, and interface motion. We also tracked the individual motion of the particles, measured the average granular temperature of the interface, and compared it with that of the whole bed. The changes in celerities suggest a regime transition on the bottom layer. The interface also presents low values of average granular temperature. Though the interface is discontinuous on the bed, the interface does not present significant changes in granular temperature.

The presence of the bottom layer seems to be hindered by the top layer, and a comparison with a monodisperse pile of some grains is still to be done. The result also suggests that both layers can not be simplified as monodisperse piles, and then the interface plays an important role in the momentum transfer to the top layer.

5. ACKNOWLEDGEMENTS

The authors are grateful to FAPESP (Grant Nos. 2018/14981-7, 2020/00221-0 and 2022/01758–3) and to CNPq (Grant No. 405512/2022-8) for the financial support provided.

6. REFERENCES

Bertho, Y., Giorgiutti-Dauphiné, F. and Hulin, J.P., 2003. "Dynamical janssen effect on granular packing with moving walls". *Phys. Rev. Lett.*, Vol. 90, p. 144301. doi:10.1103/PhysRevLett.90.144301. URL https://link.aps.org/doi/10.1103/PhysRevLett.90.144301.

Cúñez, F.D. and Franklin, E.M., 2019. "Plug regime in water fluidized beds in very narrow tubes". *Powder Technology*, Vol. 345, pp. 234–246. ISSN 0032-5910. doi:https://doi.org/10.1016/j.powtec.2019.01.009.

Cúñez, F.D. and Franklin, E.M., 2020. "Crystallization and jamming in narrow fluidized beds". *Physics of Fluids*, Vol. 32, No. 8, p. 083303. ISSN 1070-6631. doi:10.1063/5.0015410. URL https://doi.org/10.1063/5.0015410.

Goldman, D.I. and Swinney, H.L., 2006. "Signatures of glass formation in a fluidized bed of hard spheres". *Phys. Rev. Lett.*, Vol. 96, p. 145702. doi:10.1103/PhysRevLett.96.145702. URL https://link.aps.org/doi/10.1103/PhysRevLett.96.145702.

Guazzelli, , 2005. *Fluidized Beds: From Waves to Bubbles*, pp. 211 – 232. ISBN 9783527603626. doi:10.1002/352760362X.ch9.

Oliveira, V.P.S., Borges, D.S. and Franklin, E.M., 2023 (accepted). "Crystallization and reuidization in very-narrow uidized beds". *Phys. of Fluids.*

Richardson, J. and Zaki, W., 1997. "Sedimentation and fluidisation: Part i". *Chemical Engineering Research and Design*, Vol. 75, pp. S82–S100. ISSN 0263-8762. doi:https://doi.org/10.1016/S0263-8762(97)80006-8. URL https://www.sciencedirect.com/science/article/pii/S0263876297800068.

Yao, Y., Criddle, C.S. and Fringer, O.B., 2021. "Comparison of the properties of segregated layers in a bidispersed fluidized bed to those of a monodispersed fluidized bed". *Phys. Rev. Fluids*, Vol. 6, p. 084306. doi:10.1103/PhysRevFluids.6.084306. URL https://link.aps.org/doi/10.1103/PhysRevFluids.6.084306.

7. RESPONSIBILITY NOTICE

The authors are solely responsible for the printed material included in this paper.